Theory of the Photo- and Electrodisintegration of Be^9 †

EUGENE GUTH AND CHARLES J. MULLIN
University of Notre Dame, Notre Dame, Indiana
(Received February 14, 1949)

Cross sections for the photo- and electrodisintegration processes at relatively low energies have been calculated as a function of energy on the basis of a simple model of the Be^9 nucleus in which a neutron is assumed to move in the potential well provided by the remainder of the nucleus. According to the theory, the disintegration at low energies results primarily from electric dipole transitions from the ground $P_{3/2}$ state to S and D states in the positive energy continuum. Magnetic dipole disintegration does not seem to play an important role. In order to obtain agreement between the theoretical and empirical photo-disintegration cross sections, it seems necessary to make the plausible assumption that the interaction between the prospective photo-neutron and the remaining nucleons of the nucleus is a function of the orbital angular momentum of the system (Majorana interaction). Furthermore, complete neglect of the $P_{3/2}-P_{\frac{1}{2}}$ splitting of the lowest P state leads to an angular distribution of the ejected neutrons which does not agree with the (preliminary) empirical results.

Using the Born-Møller Approximation, the cross section for electrodisintegration has been calculated in terms of the photo-disintegration cross section. This method yields a correlation, which is independent of the nuclear model, between the observed photo- and electrodisintegration cross sections.

The theory based upon the simple model described seems adequate for an interpretation of the experimental data.

I. SUMMARY OF EMPIRICAL DATA ON THE DISINTEGRATION OF Be^9 BY LOW ENERGY PHOTONS, ELECTRONS, AND PROTONS

RECENTLY the cross section for the photo-disintegration of Be^9 was measured as a function of energy by Wattenberg and his associates.[1] Their results, as well as the results of other workers, are shown in Fig. 1. (The solid curve in Fig. 1 is a plot of the theoretical cross section derived in Section III of this paper.) It should be noted that the experimental results indicate that the photo-disintegration cross section has a sharp maximum and a minimum in the energy range covered by the data. Probably there is a second maximum beyond the range of these data.

Experimental data giving the cross section for electrodisintegration of Be^9 also are available. The first measurements were made by Collins, Waldman, and Guth[2] who obtained a value of $\sigma_e \cong 10^{-31}$ cm^2 with an electron beam energy of 1.73 Mev. Subsequently, Wiedenbeck,[3] using a thin Be target, determined the cross section as a function of energy in the energy range extending from the threshold to about 3 Mev.

Empirical results on the disintegration of Be^9 with protons have been obtained by Davis and Hafner.[4] These workers studied the energy distribution of protons inelastically scattered on Be^9. Incident proton energies of 4.5 Mev and 7.1 Mev were used, and the protons scattered through 37° were analyzed. The results show a sharp maximum in the energy distribution curve at 2.41 Mev.

The purpose of the present work is to see if the photo- and electrodisintegration data can be explained on the basis of a simple model of the Be^9 nucleus. The theory of the disintegration of Be^9 by protons has been given by Longmire.[5] Only a brief discussion of the correlation between the data on proton disintegration and those on photo- and electrodisintegration is given in this paper.

II. THE MODEL FOR THE Be^9 NUCLEUS

A. The Ground State

Three models for the Be^9 nucleus have been investigated.[6] These are: (1) the Hartree model, (2) the α-particle model ($2\alpha+n$), and (3) an "equivalent two-body model" in which the two α-particles are treated as a unit (Be^8) and the remaining neutron is assumed to move in the field of the Be^8 nucleus. Calculations to determine the ground state and magnetic moment of Be^9 have been carried out on the bases of the Hartree and α-particle approximations.[7-9] These calculations predict a $^2P_{3/2}$ ground state, and that the magnetic moment should lie in the interval $-0.7>\mu>-1.5$ nuclear magnetons.

The molecular beam magnetic resonance method has been applied to the measurement of the magnetic moment of Be^9 by Kusch, Millman, and Rabi.[10] The most reasonable interpretation of the results of these experiments yields $\mu=-1.18$ nuclear magnetons and $j=\frac{3}{2}$. An attempt to determine the angular momentum from hyperfine structure data has been made by Paul;[11] these data favor the value $j=\frac{3}{2}$ but do not exclude $j=\frac{1}{2}$.

The combined results of theory and experiment seem to favor a $P_{3/2}$ ground state, with the $D_{3/2}$ as second choice. The calculations made in this paper are based upon the choice of a $P_{3/2}$ ground state; however, the

† A statement of some of the results of the theory has been given by E. Guth and C. J. Mullin, Phys. Rev. **74**, 833 (1948), and Guth, Mullin, and Marshall, Phys. Rev. **74**, 834 (1948).

[1] Russell, Sachs, Wattenberg, and Fields, Phys. Rev. **73**, 545 (1948). The experimental data given in Fig. 1 were kindly communicated to us by Dr. Wattenberg.

[2] Collins, Waldman, and Guth, Phys. Rev. **55**, 875 (1939).

[3] Marcellus L. Wiedenbeck, Phys. Rev. **69**, 236 (1945).

[4] K. E. Davis and M. Hafner, Phys. Rev. **73**, 1473 (1948).

[5] Conrad L. Longmire, Phys. Rev. **74**, 1773 (1948); and thesis, University of Rochester, 1948. The authors wish to thank Dr. Longmire and Professor Marshak for communicating their results to us.

[6] For a brief summary of the models investigated for Be^9 see E. Guth and C. J. Mullin, Phys. Rev. **74**, 832 (1948).

[7] E. Feenberg and E. Wigner, Phys. Rev. **51**, 95 (1937).

[8] M. E. Rose and H. A. Bethe, Phys. Rev. **51**, 205 (1937).

[9] Robert G. Sachs, Phys. Rev. **55**, 825 (1939).

[10] Kusch, Millman, and Rabi, Phys. Rev. **55**, 666 (1939).

[11] W. Paul, Zeits. f. Physik **117**, 774 (1941).

empirical data probably can be explained also on the basis that the ground state is a $D_{3/2}$ state.

B. The Equivalent Two-Body Model

Attempts to calculate the disintegration cross sections on the basis of either the Hartree approximation or the α-particle approximation lead, of course, to laborious computations. For this reason a simpler yet creditable model of the Be^9 nucleus is desirable. In the Be^9 nucleus one neutron is loosely bound, having a binding energy of about 1.63 Mev,[12] compared to the 8–10-Mev average binding energy per particle. Guth[13] first pointed out that this would lend credence to the simple two-body model in which the neutron is regarded as moving in the potential field of the Be^8 nucleus. Although the Be^8 nucleus is unstable, breaking down into two α-particles, the unstability is only 116 kev;[14] and the lifetime of Be^8 is long compared to the time required for the ejection of a neutron from Be^9. Consequently, it may be expected that the two-body model is a reasonable approximation for the explanation of at least the coarse features of the disintegration process at low energies where only neutron ejection occurs. At higher energies competing processes, involving the ejection of a proton or an α-particle ($Be^9 \rightarrow He^5 + He^4$) may be expected.[15] For the description of these processes, and for an accurate description of the properties of the Be^9 nucleus (e.g., magnetic moment), a more accurate model is required.[16]

C. The Be^8-Neutron Interaction

In the present work the Be^8-neutron interaction for a given eigenstate of the system is assumed to be of the central field (non-tensor) type; for simplicity, this central interaction is represented by a spherical potential well. If the interaction is solely of the "ordinary" type, one well should describe the interaction for all the eigenstates of the system. If, on the other hand, the interaction is partly of the exchange type, the interaction energy may be expected to be a function of the orbital angular momentum of the system and of the orientation of the spin of the neutron. Since the Be^8 nucleus presumably has spin zero, it seems likely that the resultant of the interaction between the spin of the neutron and the spins of the Be^8 nucleons is small and plays a role only in the "fine structure" of the energy levels corresponding to a given value of the orbital angular momentum. Majorana-type forces, on the other hand, may be large; thus, the well depth and the well radius may be a function of the orbital angular momentum or at least of parity.

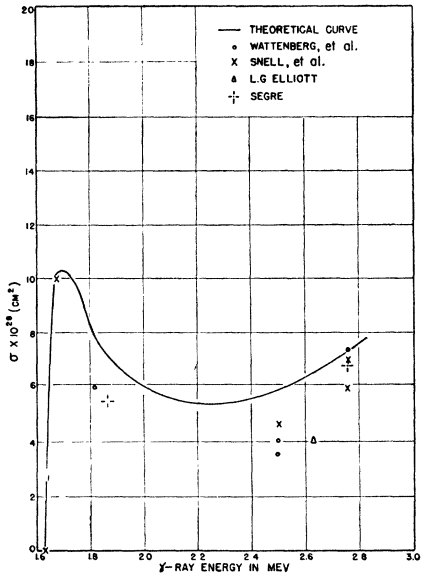

FIG. 1. Photo-disintegration cross sections for Be^9.

The assumption that the Be^8-neutron interaction is of the "ordinary" type, requiring only one well to describe the interactions for all states of the system, has been employed by Mamasachlisov[17] in formulating a theory of the electrodisintegration of Be^9. The disintegration is attributed to an electric dipole transition from the ground P state to an S state in the positive energy continuum. Mamasachlisov's results, which were based in part on the results of Bethe and Peierls[18] for the electrodisintegration of the deuteron, appeared to give good agreement with the experimental measurements of Collins, Waldman, and Guth at 1.73 Mev. However, the results of Bethe and Peierls used by Mamasachlisov were marred by two algebraic errors which were subsequently corrected by Wick.[19] The correction of these errors reduced Mamasachlisov's theoretical cross section

[12] The calculations in this paper are based upon the value 1.63 for the binding energy of the neutron. This value was determined by Collins, Waldman, and Guth (reference 2). More recent measurements on the binding energy of the deuteron by R. E. Bell and L. G. Elliott (Phys. Rev. **74**, 1552 (1948)) yield a value of about 1.67 Mev for the binding energy of the neutron in Be^9. Use of this latter value would not greatly alter our results for the total cross section, but may, of course, alter the angular distribution of the photo-neutrons by a measureable amount at some γ-ray energies.

[13] Eugene Guth, Phys. Rev. **55**, 411 (1939).

[14] The instability was first shown by E. Glückauf and F. A. Paneth, Proc. Roy. Soc. **A165**, 229 (1938). The value 116 kev is due to Arthur Hemmendinger, Phys. Rev. **73**, 806 (1948).

[15] The $\gamma - p$ reaction for Be^9 has been observed by Ogle, Brown, and Conklin, Phys. Rev. **71**, 378 (1947) and Phys. Rev. **73**, 648 (1948); the threshold for proton ejection is about 18 Mev. The threshold for the ejection of an α-particle ($Be^9 \rightarrow He^5 + H^4$) and the threshold for the $Be^9 \rightarrow \alpha + \alpha + n$ process should be about 5 Mev.

[16] T. Schmidt (Zeits. f. Physik **106**, 358 (1937)) has used the two-body model to explain the magnetic moments of nuclei. As expected, the representation is better for medium and heavy nuclei than it is for light nuclei. Inclusion of the exchange current contribution to the magnetic moment yields only a small correction to Schmidt's results. A general theoretical discussion of the magnetic moments of nuclei has also been given by Margenau and Wigner (Phys. Rev. **58**, 103 (1940)). Assuming the ground state of Be^9 to be a $P_{3/2}$ state, the measurements of Kusch, Millman, and Rabi (reference 10) yield a result for the magnetic moment which falls above the lower limits set by these theories, and which is, therefore, consistent with the results obtained from these theories.

[17] V. I. Mamasachlisov, J. Phys. U.S.S.R. **7**, 239 (1943).

[18] H. A. Bethe and R. Peierls, Proc. Roy. Soc. **A148**, 146 (1935).

[19] G. C. Wick, Ricerca Scient. **11**, 49 (1940). See also B. Peters and C. Richman, Phys. Rev. **59**, 804 (1941).

by a factor of about one-half and led to a less favorable comparison with the experimental result. Caldirola[20] tried to improve Mamasachlisov's theory by introducing, *ad hoc*, a magnetic dipole transition between the $P_{3/2}$ ground state and a $P_{\frac{1}{2}}$ state in the positive energy continuum; again all states were assumed to be eigenstates of the same potential well. However, if the $P_{3/2}$ and $P_{\frac{1}{2}}$ states belong to the same potential well, the magnetic dipole cross section vanishes. Caldirola apparently did not notice this and, using approximations, obtained a non-zero value for a vanishing integral.

Interaction of the "ordinary" type has also been applied to the theory of the photo-disintegration of Be^9 by Mamasachlisov,[21] Borsellino,[22] and Schlögl.[23] These workers consider a $P \rightarrow S$ transition. Unfortunately the virtual level of the S state belonging to the same well as the ground P state is far too broad and occurs at too high an energy to explain the rather sharp maximum which occurs just above the threshold in the empirical cross section *versus* energy curve. Furthermore, it seems that *two* transitions are required to explain the maximum, minimum, and subsequent rise in the experimental curve (Fig. 1).

It should be noted that the assumption that the Be^8-neutron interaction is entirely of the "ordinary type" contradicts the assumption that the ground state is a P state. For if the S states belong to the same well as the P states, the lowest lying bound level should be an S state. Furthermore, application of the Pauli principle to the external neutron and those in the α-particles makes it seem likely that the effective potential is deeper for P states than it is for S and D states. Because of these considerations, and since the positive energy states belonging to the potential well used to describe the ground state have virtual levels which (1) are far too broad and (2) do not occur at the proper energy values

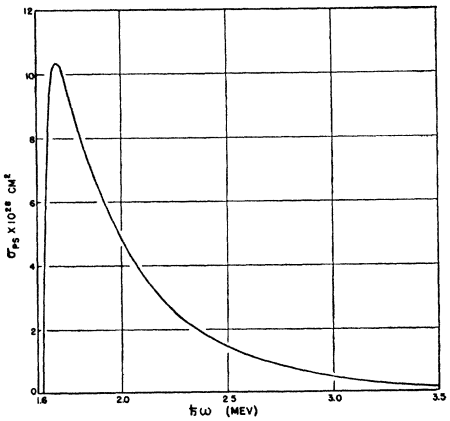

FIG. 2. Photo-disintegration cross sections due to the $P \rightarrow S$ transitions.

to explain the empirical data, it seems necessary to assume that the Be^8-neutron interaction is of a type which depends upon the orbital angular momentum (or at least upon parity) and upon the orientation of the spin of the neutron. In the spherical potential well approximation, this type of interaction is introduced schematically by assuming the well depth to be a function of orbital angular momentum and spin orientation. The spin interaction results in a "fine structure" splitting of the levels corresponding to a given value of the orbital angular momentum. Thus, presumably, the ground P state is split into $P_{3/2}$ and $P_{\frac{1}{2}}$ levels, with the $P_{3/2}$ level as the ground state. This inverted order of the splitting would be expected if the spin interaction is of the relativistic spin-orbit type. Although there is no conclusive experimental evidence for the splitting of the lowest P state in Be^9, it is reasonable to assume this splitting to be approximately the same as the known splitting of similar levels in other light nuclei. In He^5 the ^2P splitting is about 250 kev[24] and appears to be normal —the ground state being a $P_{\frac{1}{2}}$ state. Dancoff[25] has shown that this splitting may be understood on the basis of tensor forces. In Li^7 an excited state has been found 478.5 kev above the ground state.[26] The ground state for Li^7 is believed to be a $P_{3/2}$ state. Until recently it has been assumed that the excited state 478.5 kev above the ground state is the $P_{\frac{1}{2}}$ member of the P doublet, the 478.5 kev separation probably being due to relativistic spin orbit coupling.[27] This interpretation has been successfully applied, for example, in the interpretation of the experimental data on the K-capture transitions $Be^7 \rightarrow Li^7$ and $Be^7 \rightarrow Li^{7*}$.[28] An analysis of the $B^{10}(n, \alpha)Li^7$ reaction, using the recently measured[29] value $I=3$ for the nuclear spin of B^{10}, leads Inglis[30] to favor the interpretation that the ^2P splitting is so small that it has not been resolved, and that the observed excited state is an unresolved $^2F_{7/2, 5/2}$. The magnitude of the ^2P splitting in Be^9 is not of great importance in the present work, in which it will be assumed only that the splitting is of sufficient magnitude that practically all the Be^9 nuclei are initially in the $j=\frac{3}{2}$ state. Complete neglect of the ^2P

[20] P. Caldirola, J. de phys. et rad. **8**, 155 (1947).
[21] V. I. Mamasachlisov, Physik. Zeits. Sowjetunion **9** (1936).
[22] A. Borsellino, Nuovo Cimento **5**, No. 4 (1948).
[23] F. Schlögl, Zeits. f. Naturforschung **3a**, 229 (1948). Schlögl also considers the possibility that the ground state may be an S state.
[24] H. Staub and H. Tatel, Phys. Rev. **58**, 820 (1940); H. Staub and W. E. Stephens, Phys. Rev. **55**, 131 (1939).
[25] S. M. Dancoff, Phys. Rev. **58**, 326 (1940).
[26] The value 478.5 kev is due to L. G. Elliott and R. E. Bell, Phys. Rev. **74**, 1869 (1948). The excited state was found by L. H. Rumbaugh and L. R. Hafstad, Phys. Rev. **50**, 681 (1936). Six reactions which leave Li^7 in a low lying excited state are known. These reactions have been summarized by W. Hornyak and T. Lauritsen, Rev. Mod. Phys. **20**, 191 (1948).
[27] David R. Inglis, Phys. Rev. **50**, 783 (1936) and Phys. Rev. **56**, 1178 (1939). See also G. Breit and J. R. Stehn, Phys. Rev. **53**, 459 (1938), and Charles Kittel, Phys. Rev. **62**, 109 (1942). The most recent theoretical considerations seem to indicate that relativistic spin-orbit coupling does not produce large splitting; the origin of the nuclear doublets is not understood quantitatively at present. See S. Hanna and D. R. Inglis, Phys. Rev. **75**, 1767 (1949); D. R. Inglis, Phys. Rev. **75**, 1767 (1949).
[28] C. Breit and J. K. Knipp, Phys. Rev. **54**, 652 (1938). See also Emil Jan Konopinski, Rev. Mod. Phys. **15**, 209 (1943).
[29] Gordy, Ring, and Burg, Phys. Rev. **74**, 1191 (1948). See also M. Goldhaber, Phys. Rev. **74**, 1194 (1948).
[30] David R. Inglis, Phys. Rev. **74**, 1876 (1948).

splitting seems to lead to an incorrect angular distribution for the neutrons obtained in the (γ, n) process (see Section III-*D*). In Section III-*E* it is shown that magnetic dipole transitions play a negligible role in the disintegration process if the ^2P splitting does not exceed 500 kev.

SYMBOLS USED IN THE TEXT

i: initial eigenstate of the system
f: final eigenstate of the system normalized on the energy scale
m: rest mass of the electron
M: mass of neutron
μ: reduced mass of neutron $\cong \frac{8M}{9}$
r: radius vector from Be^8 to neutron
z: $r\cos\theta$
α_n, β_n: spin eigenvectors for the neutron
$\boldsymbol{\sigma}_n$: Pauli spin vector for the neutron
$\boldsymbol{\mu}_n$: magnetic moment of neutron
ϵ: binding energy for the ground state
E: energy of the neutron
$Y_{l,m}(\theta,\phi)$: normalized surface harmonic
$j_l(x)$: spherical Bessel function of order l:

$$j_l(x)=\left(\frac{\pi}{2x}\right)^{\frac{1}{2}}J_{l+\frac{1}{2}}(x)$$

$V_{l,j}$: well-depth describing the Be^8-neutron interaction in the state with quantum numbers l (orbital angular momentum) and j (total angular momentum)
V_2: average well depth for the $D_{3/2}$, $D_{5/2}$ states

$$\alpha=\left[\frac{2\mu}{\hbar^2}\epsilon\right]^{\frac{1}{2}},\quad k=\left[\frac{2\mu}{\hbar^2}E\right]^{\frac{1}{2}},$$

$$\beta=\left[\frac{2\mu}{\hbar^2}(V_{1,3/2}+E)\right]^{\frac{1}{2}},$$

$$\gamma=\left[\frac{2\mu}{\hbar^2}(V_{0,\frac{1}{2}}+E)\right]^{\frac{1}{2}},$$

$$\xi=\left[\frac{2\mu}{\hbar^2}(V_2+E)\right]^{\frac{1}{2}},$$

$$\eta=\left[\frac{2\mu}{\hbar^2}(V_{1,\frac{1}{2}}+E)\right]^{\frac{1}{2}}.$$

III. CROSS SECTION FOR PHOTO-DISINTEGRATION

A. General Considerations

Photo-disintegration of Be^9 results when photons incident upon the nucleus cause the neutron to be excited from the ground state to states of positive energy. In general, the photons may produce photoelectric and photomagnetic transitions. In first approximation, only electric dipole and magnetic dipole transitions need be considered at low energies. Since the resultant spin interaction between the loosely bound neutron and the nucleons of Be^8 seems to be small, the well depth used to describe the Be^8 neutron interaction is only slightly dependent upon the orientation of the neutron spin; consequently, the cross section for magnetic dipole transitions is small, and, in first approximation, only electric dipole transitions need be considered. (Later, in part *E* of this section, magnetic dipole transitions will be considered.) Using a ground P state, the selection rule

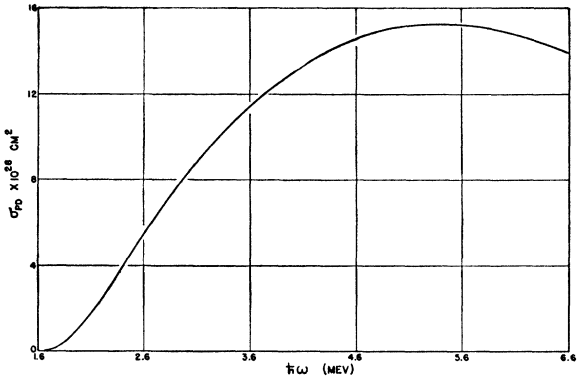

FIG. 3. Photo-disintegration cross sections due to the $P\rightarrow D$ transitions.

$\Delta l=\pm 1$ for electric dipole transitions permits $P\rightarrow S$ and $P\rightarrow D$ transitions.

The cross section for electric dipole disintegration of Be^9 is given by

$$\sigma=(64\pi^2/81)(e^2/\hbar c)\hbar\omega\sum|\langle f|z|i\rangle|^2, \tag{1}$$

where the summation is to be extended over all non-vanishing matrix elements. Assuming the spin interaction to be small and of a central (non-tensor) type, the eigenstates f, i are described by the quantum numbers E (energy), j, m_j, and l. The eigenfunctions are

$$\psi(l,\ j=l+\tfrac{1}{2},\ m_j)$$
$$=\frac{R_{l,j}(r)}{(2l+1)^{\frac{1}{2}}}\{(l+\tfrac{1}{2}+m_j)^{\frac{1}{2}}Y_{l,\,m_j-\frac{1}{2}}(\theta,\phi)\alpha_n$$
$$+(l+\tfrac{1}{2}-m_j)^{\frac{1}{2}}Y_{l,\,m_j+\frac{1}{2}}(\theta,\phi)\beta_n\}, \tag{2a}$$

$$\psi(l,\ j=l-\tfrac{1}{2},\ m_j)$$
$$=\frac{R_{l,j}(r)}{(2l+1)^{\frac{1}{2}}}\{(l+\tfrac{1}{2}-m_j)^{\frac{1}{2}}Y_{l,\,m_j-\frac{1}{2}}(\theta,\phi)\alpha_n$$
$$-(l+\tfrac{1}{2}+m_j)^{\frac{1}{2}}Y_{l,\,m_j+\frac{1}{2}}(\theta,\phi)\beta_n\}. \tag{2b}$$

The matrix element $\langle f|z|i\rangle$ of Eq. (1) is different from zero only if $\Delta l=\pm 1$, $\Delta j=0,\ \pm 1$, $\Delta m_j=0$.

B. Cross Section for the $P\rightarrow S$ Transition

Using the potential well approximation, the Be^8-neutron interaction for the ground $P_{3/2}$ state is described by

$$V=-V_{1,3/2}\quad r\leqslant r_0,$$
$$V=0\quad r\geqslant r_0.$$

The four initial states are given by Eq. (2a). For these states

$$R_{1,3/2}(r)=A_1 j_1(\beta r)\quad r\leqslant r_0,$$
$$R_{1,3/2}(r)=B_1\frac{(1+\alpha r)}{r^2}e^{-\alpha(r-r_0)}\quad r\geqslant r_0, \tag{3}$$

with

$$B_1=-\frac{A_1}{\alpha^2}\sin\beta r_0, \tag{4a}$$

$$\beta r_0\cot\beta r_0=1+(1+\alpha r_0)\left(\frac{\beta}{\alpha}\right)^2, \tag{4b}$$

$$\frac{A_1^2 r_0}{2\beta^2}\left\{1+\left[(2+\alpha r_0)\left(\frac{\beta}{\alpha}\right)^4+(1+\alpha r_0)\left(\frac{\beta}{\alpha}\right)^2-1\right]\frac{\sin^2\beta r_0}{(\beta r_0)^2}\right\}=1. \tag{4c}$$

Using $\epsilon=1.63$ Mev, and assuming $r_0=5\times10^{-13}$ cm, Eq. (4b) gives $V_{1,3/2}=12.16$ Mev. Equations (4a) and (4c) then determine A_1 and B_1.

The final S states are obtained from Eq. (2a) with

$$R_{0,\frac{1}{2}}=A_0 j_0(\gamma r), \qquad r\leqslant r_0,$$
$$R_{0,\frac{1}{2}}=\left(\frac{2}{\pi}\frac{\mu k}{\hbar^2}\right)^{\frac{1}{2}}\frac{\sin[k(r-r_0)+\delta_0]}{kr} \qquad r\geqslant r_0, \tag{5}$$

where

$$A_0\sin\gamma r_0=\frac{\gamma}{k}\left(\frac{2}{\pi}\frac{\mu k}{\hbar^2}\right)^{\frac{1}{2}}\sin\delta_0, \tag{6a}$$

$$A_0\cos\gamma r_0=\left(\frac{2}{\pi}\frac{\mu k}{\hbar^2}\right)^{\frac{1}{2}}\cos\delta_0. \tag{6b}$$

For the $P\rightarrow S$ transition, these equations yield

$$\sum|\langle f|z|i\rangle|^2=|R_{ps}|^2/9, \tag{7}$$

where

$$R_{ps}=\int_0^\infty R_{0,\frac{1}{2}}{}^* R_{1,3/2} r^3 dr,$$

and, thus,

$$\sigma_{ps}=(64\pi^2/729)(e^2/\hbar c)\hbar\omega|R_{ps}|^2. \tag{8}$$

From Eqs. (3), (4), (5), and (6)

$$R_{ps}=\frac{B_1\alpha^2[(2/\pi)(\mu k/\hbar^2)]^{\frac{1}{2}}}{r_0(k^2+\gamma^2\cot^2\gamma r_0)^{\frac{1}{2}}}\times\left\{\frac{2+2(\beta^2/\alpha^2)(1+\alpha r_0)-r_0^2(\gamma^2-\beta^2)}{(\gamma^2-\beta^2)^2}+\frac{\alpha r_0(2+\alpha r_0)+k^2r_0^2}{(\alpha^2+k^2)^2}+\left[-\frac{2+[(\gamma^2-\beta^2)/\alpha^2](1+\alpha r_0)}{(\gamma^2-\beta^2)^2}+\frac{3+\alpha r_0+(k^2/\alpha^2)(1+\alpha r_0)}{(\alpha^2+k^2)^2}\right]\cdot\gamma r_0\cot\gamma r_0\right\} \tag{9}$$

with B_1 given by Eq. (4).

The cross section given by Eq. (8) contains the well depth $V_{0,\frac{1}{2}}$ as an adjustable parameter.[31] The choice $V_{0,\frac{1}{2}}=3$ Mev yields the curve shown in Fig. 2. The cross section for the $P\rightarrow S$ transition gives a sharp maximum* just above the threshold and is in fairly good agreement with the experimental measurements made for energies just above the threshold (Fig. 1).

C. Cross Section for the $P\rightarrow D$ Transition

The wave functions for the final $D_{3/2}$ and $D_{5/2}$ states are given by Eq. (2). The gradual rise beyond 2.5 Mev in the cross section *versus* energy curve is presumably due to the $P\rightarrow D$ transition. The gradualness of this rise indicates that the resonance D levels are broad. If the resonance D levels are broad, and if the $D_{5/2}-D_{3/2}$ splitting is not unexpectedly large, a good approximation is obtained by using the same (average) well to describe the $D_{3/2}$ and $D_{5/2}$ states. (This means that in the evaluation of σ_{PD} we set $V_{2,3/2}=V_{2,5/2}=V_2=$average well depth describing the Be^8-neutron interaction in the D-state.) Using this approximation,

$$R_{2,3/2}=R_{2,5/2}=R_2=A_2 j_2(\xi r),$$
$$R_{2,3/2}=R_{2,5/2}=R_2=\left(\frac{2}{\pi}\frac{\mu k}{\hbar^2}\right)^{\frac{1}{2}}\frac{(3-k^2r^2)\sin[k(r-r_0)+\delta_2]-3kr\cos[k(r-r_0)+\delta_2]}{k^3r^3}, \tag{10}$$

with

$$A_2=\left(\frac{2}{\pi}\frac{\mu k}{\hbar^2}\right)^{\frac{1}{2}}\left(\frac{\xi}{k}\right)^3\times\frac{(3-k^2r_0^2)\sin\delta_2-3kr_0\cos\delta_2}{(3-\xi^2r_0^2)\sin\xi r_0-3\xi r_0\cos\xi r_0}, \tag{11a}$$

$$\frac{(3-k^2r_0^2)\sin\delta_2-3kr_0\cos\delta_2}{(3-\xi^2r_0^2)\sin\xi r_0-3\xi r_0\cos\xi r_0}=\left(\frac{k}{\xi}\right)^2\frac{\sin\delta_2-kr_0\cos\delta_2}{\sin\xi r_0-\xi r_0\cos\xi r_0}; \tag{11b}$$

thus for the $P_{3/2}\rightarrow D_{3/2}$ transition

$$\sum|\langle f|z|i\rangle|^2=\frac{|R_{PD}|^2}{250}\int\{[4|Y_{22}|^2+|Y_{21}|^2]+\tfrac{1}{9}[2|Y_{20}|^2+3|Y_{21}|^2]\}d\Omega \tag{12a}$$
$$=\frac{|R_{PD}|^2}{45}; \tag{12b}$$

[31] Since the well depth and well radius are not independent parameters, the same well radius, $r_0=5\times10^{-13}$ cm, has been used for all wells.

* The choice $V_{0,\frac{1}{2}}=3$ Mev for the depth of the S-well yields a bound level at $E\cong-100$ kev. This level acts as a *resonance* level,

and for the $P_{3/2}\rightarrow D_{5/2}$ transition

$$\sum|\langle f|z|i\rangle|^2=\frac{|R_{PD}|^2}{125}\int\{2[4|Y_{21}|^2+|Y_{22}|^2]$$
$$+3[3|Y_{20}|^2+2|Y_{21}|^2]\}d\Omega \quad (13a)$$
$$=\frac{|R_{PD}|^2}{5}, \quad (13b)$$

where

$$R_{PD}=\int_0^\infty R_2^* R_{1,3/2} r^3 dr.$$

The term in the first bracket on the right-hand side of each of the Eqs. (12a) and (13a) represents the contribution from the $|m_j|=\frac{3}{2}$ states; the term in the second bracket represents the contribution from the $|m_j|=\frac{1}{2}$ states. Adding the contributions from the $P_{3/2}\rightarrow D_{3/2}$ and the $P_{3/2}\rightarrow D_{5/2}$ transitions, the cross section for transition to the D doublet is

$$\sigma_{PD}=\frac{128}{729}\pi^2\frac{e^2}{\hbar c}\hbar\omega|R_{PD}|^2. \quad (14)$$

From Eqs. (3), (4), (10), and (11)

$$R_{PD}=\frac{B_1[(2/\pi(\mu k/\hbar^2))^{\frac{1}{2}}}{\{k^2r_0^2(3QP+k^2r_0^2)^2+(3QP+k^2\xi r_0^3\cot\xi r_0)^2\}^{\frac{1}{2}}}$$
$$\times\left\{k^2r_0^2\left[\frac{2k^2(1+\alpha r_0)-\alpha^2r_0^2(\alpha^2+k^2)}{(\alpha^2+k^2)^2}\right.\right.$$
$$\left.-\frac{2(1+\alpha r_0)\xi^2-\alpha^2r_0^2(\xi^2-\beta^2)}{(\xi^2-\beta^2)^2}\right]$$
$$+k^2r_0^2Q\left[\frac{(\alpha^2+k^2)(1+\alpha r_0+3(\alpha^2/k^2))+2\alpha^2}{(\alpha^2+k^2)^2}\right.$$
$$\left.-\frac{(\xi^2-\beta^2)(1+\alpha r_0+(\alpha^2/\xi^2))+2\alpha^2}{(\xi^2-\beta^2)^2}\right]$$
$$\left.+3PQ\left[\frac{2k^2(1+\alpha r_0)-\alpha^2r_0^2(\alpha^2+k^2)}{(\alpha^2+k^2)^2}\right]\right\}, \quad (15)$$

where $Q=1-\xi r_0\cot\xi r_0$ and $P=1-\xi^2/k^2$. The cross section σ_{PD} contains the well depth $V_2(=V_{2,3/2}=V_{2,5/2})$ as an adjustable parameter. However, on the basis of a Majorana interaction, it may be expected that the well depth should be a function of parity rather than orbital angular momentum. For this reason, the choice $V_2=V_{0,\frac{1}{2}}=3$ Mev has been made. With this choice, Eq. (14) yields the curve shown in Fig. 3.

maximizing the wave function inside the well; this resonance level is responsible for the sharp maximum in σ_{ps}. The photoelectric disintegration cross section of the deuteron has a *broad* maximum because the outgoing P-wave is a free wave.

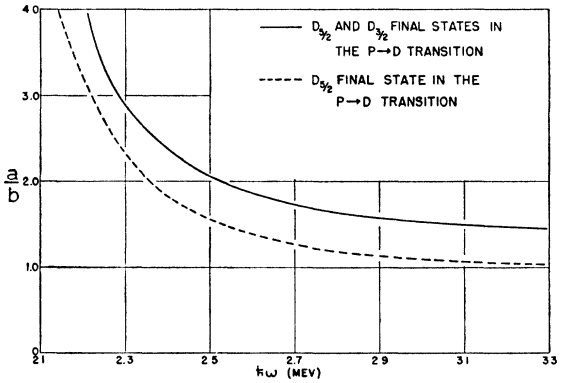

FIG. 4. Angular distribution of the photo-neutrons as a function of energy.

D. Total Cross Section for Photoelectric Disintegration

Angular Distribution of the Photo-Neutrons

In the dipole approximation, the total cross section for photoelectric disintegration is given by

$$\sigma=\sigma_{PS}+\sigma_{PD}. \quad (16)$$

The partial cross sections σ_{PS} and σ_{PD} are given by Eqs. (8) and (14). For the case $V_{0,\frac{1}{2}}=V_2=3$ Mev, the partial cross sections may be obtained from Figs. 2 and 3. For this case the resulting total cross section is plotted as the solid curve in Fig. 1. From these figures it may be seen that the $P\rightarrow S$ transition is predominant for energies near the threshold, whereas the $P\rightarrow D$ transition plays the predominant role for energies somewhat above 2.5 Mev.

In the range of energy for which the $P\rightarrow S$ transition is primarily responsible for the disintegration, the angular distribution of the ejected neutrons should be that characteristic of an S wave—spherically symmetric. In the range of energy in which the $P\rightarrow D$ transition is important, the angular distribution of the D neutrons must be taken into consideration. The angular distribution of the neutrons ejected into D states may be obtained from Eqs. (12a), (13a), and (1). The $P_{3/2}\rightarrow D_{5/2,3/2}$ cross section for ejection of a neutron into unit solid angle at θ is

$$\frac{d\sigma_{PD}}{d\Omega}=\frac{d}{d\Omega}(\sigma_{P_{3/2}\rightarrow D_{3/2}}+\sigma_{P_{3/2}\rightarrow D_{5/2}})$$
$$=\frac{\sigma_{PD}}{100\pi}(17+24\cos^2\theta). \quad (17)$$

The angle, θ, between the direction of the outgoing neutron and the direction of polarization of the incident radiation may be expressed in terms of the angle, Θ, between the direction of the outgoing neutron and the direction of propagation of the incident photon beam, and an angle, χ, giving the direction of polarization of the incident radiation:

$$\cos^2\theta=\cos^2\chi\sin^2\Theta.$$

Averaging over-all directions of polarization, $\langle\cos^2\chi\rangle_{Av}=\frac{1}{2}$, and

$$(d\sigma_{PD}/d\Omega)=(\sigma_{PD}/100\pi)(17+12\sin^2\Theta). \quad (18)$$

Adding the results due to the $P\rightarrow S$ and $P\rightarrow D$ transitions, the cross section for ejection of a neutron into unit solid angle at Θ is

$$\frac{d\sigma}{d\Omega}=\frac{\sigma_{PS}}{4\pi}+\frac{\sigma_{PD}}{100\pi}(17+12\sin^2\Theta)$$

$$=\frac{1}{4\pi}\left(\sigma_{PS}+\frac{17}{25}\sigma_{PD}+\frac{12}{25}\sigma_{PD}\sin^2\Theta\right). \quad (19)$$

The distribution is, thus, of the general form

$$d\sigma/d\Omega=a+b\sin^2\Theta, \quad (20)$$

where a and b are, of course, functions of energy. From Eq. (19)

$$\frac{a}{b}=\frac{25}{12}\frac{\sigma_{PS}}{\sigma_{PD}}+\frac{17}{12}. \quad (21)$$

The values of σ_{PS} and σ_{PD} may be calculated from Eqs. (8) and (14). For the special case that $V_{0,\frac{1}{2}}=V_2=3$ Mev, the values of σ_{PS} and σ_{PD} may be taken from Figs. 2 and 3; The resulting values for a/b are shown in Fig. 4 (solid curve). For energies just above the threshold, $\sigma_{PS}\gg\sigma_{PD}$, and the distribution is spherically symmetric; this is in agreement with the measurements of Goloborodko and Rosenkewitch[32] who found the neutrons ejected with very low energies to have a uniform angular distribution. Hamermesh and Wattenberg[33] find $a/b\cong 1.5$ at 2.76 Mev. The theoretical value obtained from Fig. 5 is $a/b=1.65$ at this energy.

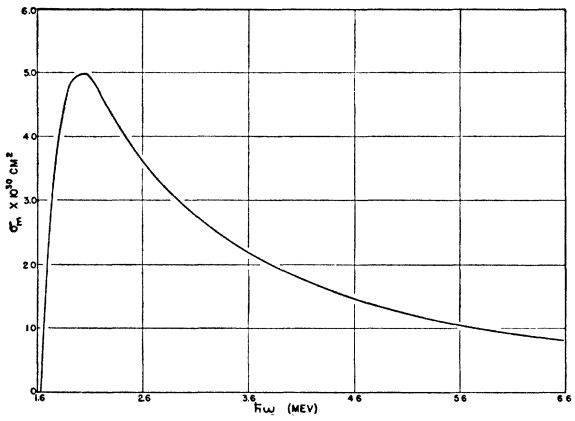

FIG. 5. Cross section for magnetic dipole disintegration.

If the splitting of the levels corresponding to a given orbital angular momentum into $j=l\pm\frac{1}{2}$ components is neglected entirely, so that the ground state has coincident $P_{3/2}$ and $P_{\frac{1}{2}}$ levels, the wave functions are

$$\psi_{E,\,l,\,m}=Y_{l,\,m}(\theta,\,\phi)R_{E,\,l}(r). \quad (22)$$

These wave functions lead to the same total cross section obtained with the wave functions given by Eq. (2). However, the angular distribution obtained from the wave functions given by Eq. (22) is

$$d\sigma/d\Omega=1/8\pi\{2\sigma_{PS}+\sigma_{PD}+\tfrac{3}{2}\sigma_{PD}\sin^2\Theta\}. \quad (23)$$

This gives the value

$$\frac{a}{b}=\frac{2}{3}\left(1+\frac{2\sigma_{PS}}{\sigma_{PD}}\right). \quad (24)$$

At 2.76 Mev, this yields $a/b=0.72$, which compares very unfavorably with the measured value of $a/b=1.5$.

Of course, another reasonable alternative is to assume that the $P_{3/2}\rightarrow D$ transition which is responsible for the rise observed beyond 2.5 Mev in the σ *versus* $\hbar\omega$ curve (Fig. 1) occurs to only one of the $D_{5/2}$, $D_{3/2}$ components. On the basis of relativistic spin orbit coupling, the $D_{5/2}$ level should occur at a lower energy than the $D_{3/2}$. The assumption that the $D_{5/2}$ level is the one primarily responsible for the $P_{3/2}\rightarrow D$ transition in the energy range of the observed data produces little change in the total cross section; actually $\sigma_{PD_{5/2}}=(9/10)\sigma_{PD}$, where σ_{PD} is given by Eq. (14). However, the angular distribution becomes

$$d\sigma/d\Omega=1/4\pi\{\sigma_{PS}+\tfrac{3}{5}\sigma_{PD_{5/2}}+\tfrac{3}{5}\sigma_{PD_{5/2}}\sin^2\Theta\}, \quad (25)$$

or

$$\frac{a}{b}=1+\frac{5}{3}\frac{\sigma_{PS}}{\sigma_{PD_{5/2}}}. \quad (26)$$

A plot of Eq. (26) for the special case $V_{0,\frac{1}{2}}=V_2=3$ Mev is given in Fig. 4 (dashed curve).

E. Magnetic Dipole Disintegration

The cross section for magnetic dipole disintegration is

$$\sigma_m=(4\pi^2/\hbar c)\hbar\omega\sum|\langle f|\mu_z|i\rangle|^2, \quad (27)$$

where the summation is to be extended over all non-vanishing matrix elements. μ_z is the component of the magnetic dipole moment of the Be^9 system along the direction of the magnetic vector of the incident radiation. The magnetic dipole moment is

$$\boldsymbol{\mu}=(e\hbar/2Mc)(\mu_n\boldsymbol{\sigma}_n+(1/18)\mathbf{L}). \quad (28)$$

The first term on the right-hand side gives the magnetic moment of the loosely bound neutron, and the second term gives the magnetic moment due to the orbital motion of the Be^8 around the center of gravity. In terms

[32] T. Goloborodko and L. Rosenkewitch, Physik. Zeits. Sowjetunion **11**, 78 (1936). See also J. Chadwick and M. Goldhaber, Proc. Roy. Soc. **A151**, 479 (1935).

[33] B. Hamermesh and A. Wattenberg, Phys. Rev. **75**, 1290(A) (1949). The value $a/b=1.5$ was obtained in a preliminary measurement. In more recent measurements B. Hamermesh, M. Hamermesh, and A. Wattenberg (scheduled for publication in Phys. Rev. Aug. 15, 1949) obtained $a/b=1.22$. E. P. Meiners (private communication) has obtained the value $a/b=1.15\pm0.07$. A more complete discussion of the theory of the angular distribution, in which the dependence of a/b upon the binding energy of the neutron is considered, has been given by C. J. Mullin and E. Guth (to be published in Phys. Rev. August 15, 1949).

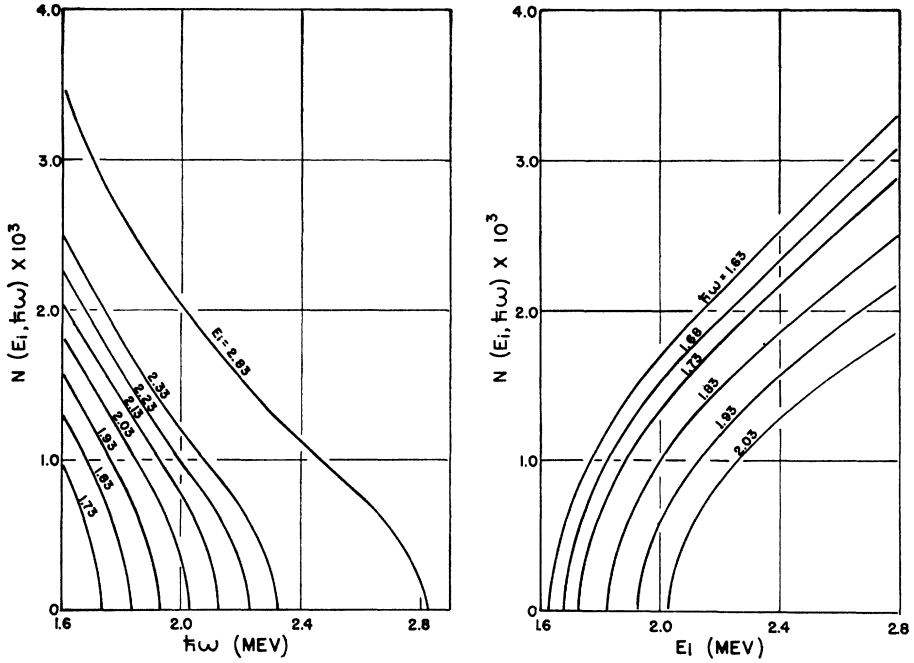

FIG. 6. Number of photoelectric quanta as a function of $\hbar\omega$ and E_i.

of the total angular momentum, $\mathbf{J}=\mathbf{L}+\frac{1}{2}\boldsymbol{\sigma}$,

$$\mu_z=\frac{e\hbar}{2Mc}\left(\mu_n-\frac{1}{36}\right)+\frac{e\hbar}{2Mc}\cdot\frac{1}{18}J_z. \tag{29}$$

Assuming the spin interaction to be relatively small and of a central (non-tensor) type, the eigenstates f, i are given by Eq. (2). For these eigenstates, J_z is a constant of the motion, and the matrix elements involving J_z vanish. Consequently,

$$\sigma_m=4\pi^2\left(\frac{e^2}{\hbar c}\right)\left(\frac{\hbar}{2Mc}\right)^2\times\left(\mu_n-\frac{1}{36}\right)^2\hbar\omega\sum|\langle f|\sigma_{nz}|i\rangle|^2. \tag{30}$$

Since the initial states are $P_{3/2}$ states, the orthogonality of the angular functions involved in f, i, requires that the final states be $P_{\frac{1}{2}}$ states if the matrix elements in Eq. (30) are to be different from zero. Obtaining f, i from Eq. (2),

$$\frac{d\sigma_m}{d\Omega}=\frac{16\pi^2}{27}\left(\frac{e^2}{\hbar c}\right)\left(\frac{\hbar}{2Mc}\right)^2\times\left(\mu_n-\frac{1}{36}\right)^2\hbar\omega|R_{PP}|^2\{|Y_{10}|^2+2|Y_{11}|^2\}, \tag{31}$$

and

$$\sigma_m=\frac{16\pi^2}{9}\left(\frac{e^2}{\hbar c}\right)\left(\frac{\hbar}{2Mc}\right)^2\hbar\omega|R_{PP}|^2, \tag{32}$$

where

$$R_{PP}=\int_0^\infty R_{1,3/2}{}^*R_{1,\frac{1}{2}}r^2dr.$$

The radial function $R_{1,3/2}$ is given by Eqs. (3) and (4). The radial function $R_{1,\frac{1}{2}}$ is

$$R_{1,\frac{1}{2}}(r)=A_{\frac{1}{2}}j_1(\eta r), \qquad r\leqslant r_0,$$
$$R_{1,\frac{1}{2}}=\left(\frac{2}{\pi}\frac{\mu k}{\hbar^2}\right)^{\frac{1}{2}}\frac{\sin[k(r-r_0)+\delta_{\frac{1}{2}}]-kr\cos[k(r-r_0)+\delta_{\frac{1}{2}}]}{k^2r^2}, \qquad r\geqslant r_0, \tag{33}$$

with

$$A_{\frac{1}{2}}=\frac{\eta^2}{k^2}\left(\frac{2}{\pi}\frac{\mu k}{\hbar^2}\right)^{\frac{1}{2}}\frac{\sin\delta_{\frac{1}{2}}-kr_0\cos\delta_{\frac{1}{2}}}{\sin\eta r_0-\eta r_0\cos\eta r_0}, \tag{34a}$$

$$\sin\delta_{\frac{1}{2}}=\frac{kr_0}{\{(kr_0)^2+[1-(k^2/\eta^2)G]^2\}^{\frac{1}{2}}}, \tag{34b}$$

$$G=1-\eta r_0\cot\eta r_0.$$

R_{PP} may be determined by straightforward integration, which gives[34]

[34] A different formula for the integral must be applied for the case $\eta=\beta$. The integration shows that the cross section does not become large for this case; in fact, this point fits on the curve obtained from (35) by excluding the point $\beta=\eta$. The same procedure must be applied to Eqs. (9) and (15); however with these equations, the singular point occurs for energies far outside the range of interest to us.

$$\sigma_m=\frac{16\pi}{9}\frac{e^2}{\hbar c}\left(\frac{\hbar}{2Mc}\right)^2\left(\mu_n-\frac{1}{36}\right)^2 B_1^2\cdot\frac{k^3}{\alpha^2+k^2}$$
$$\frac{(1+\alpha r_0+(\alpha^2/\eta^2)G)^2[(\alpha^2+k^2/\beta^2-\eta^2)+1]^2}{(kr_0)^2+(1-(k^2/\eta^2)G^2)} \quad (35)$$

with B_1 given by Eq. (4). The equation for σ_m contains $V_{1,\frac{1}{2}}$, the well depth describing the Be^8-neutron interaction in the $P_{\frac{1}{2}}$ state, as an adjustable parameter. The last factor in the numerator of Eq. (35) may be written:

$$\left(\frac{\alpha^2+k^2}{\beta^2-\eta^2}+1\right)^2=\left(\frac{V_{1,3/2}-V_{1,\frac{1}{2}}}{E+\epsilon}\right)^2 \times\left(1-\frac{V_{1,3/2}-V_{1,\frac{1}{2}}}{E+\epsilon}\right)^{-2}. \quad (36)$$

The quantity $V_{1,3/2}-V_{1,\frac{1}{2}}$ is determined by the splitting of the $P_{3/2}$ and $P_{\frac{1}{2}}$ components of the *lowest* bound P level. If this splitting is small

$$\frac{V_{1,3/2}-V_{1,\frac{1}{2}}}{E+\epsilon}\ll 1,$$

and

$$\left(\frac{\alpha^2+k^2}{\beta^2-\eta^2}+1\right)\cong\left(\frac{V_{1,3/2}-V_{1,\frac{1}{2}}}{E+\epsilon}\right)^2. \quad (37)$$

Consequently, if the $P_{3/2}-P_{\frac{1}{2}}$ splitting of the lowest P level is neglected, that is, if the same well is used to represent the $P_{3/2}$ and $P_{\frac{1}{2}}$ states, σ_m vanishes. A reasonable upper limit for the splitting of the $P_{3/2}$ and $P_{\frac{1}{2}}$ components of the lowest bound P level is 500 kev (see Section II C). Using $\epsilon=1.63$ for the binding energy in the $P_{3/2}$ ground state, and using a 500 kev splitting, Eq. (4b) gives $V_{1,3/2}=12.16$ Mev and $V_{1,\frac{1}{2}}=9.84$ Mev. The use of these values should give an upper limit for σ_m. The magnetic dipole cross section obtained by using these values for the well depths is shown in Fig. 5. It may be seen that over the energy range for which the basic assumptions of the theory are valid the magnetic dipole cross section is much smaller than the electric dipole cross section.

Equation (31) shows that the neutrons obtained by photomagnetic disintegration should have a uniform angular distribution.

IV. CROSS SECTION FOR ELECTRODISINTEGRATION

Since the electrodisintegration is accomplished by quanta emitted by the incident electrons, the electrodisintegration cross section, σ_e, may be expressed in terms of the photo-disintegration cross section, $\sigma(\hbar\omega)$. Guth[14] applied this method to the calculation of the electrodisintegration cross section for Be^9 for energies just above the threshold and obtained a value which agrees reasonably well with the value observed at 1.73

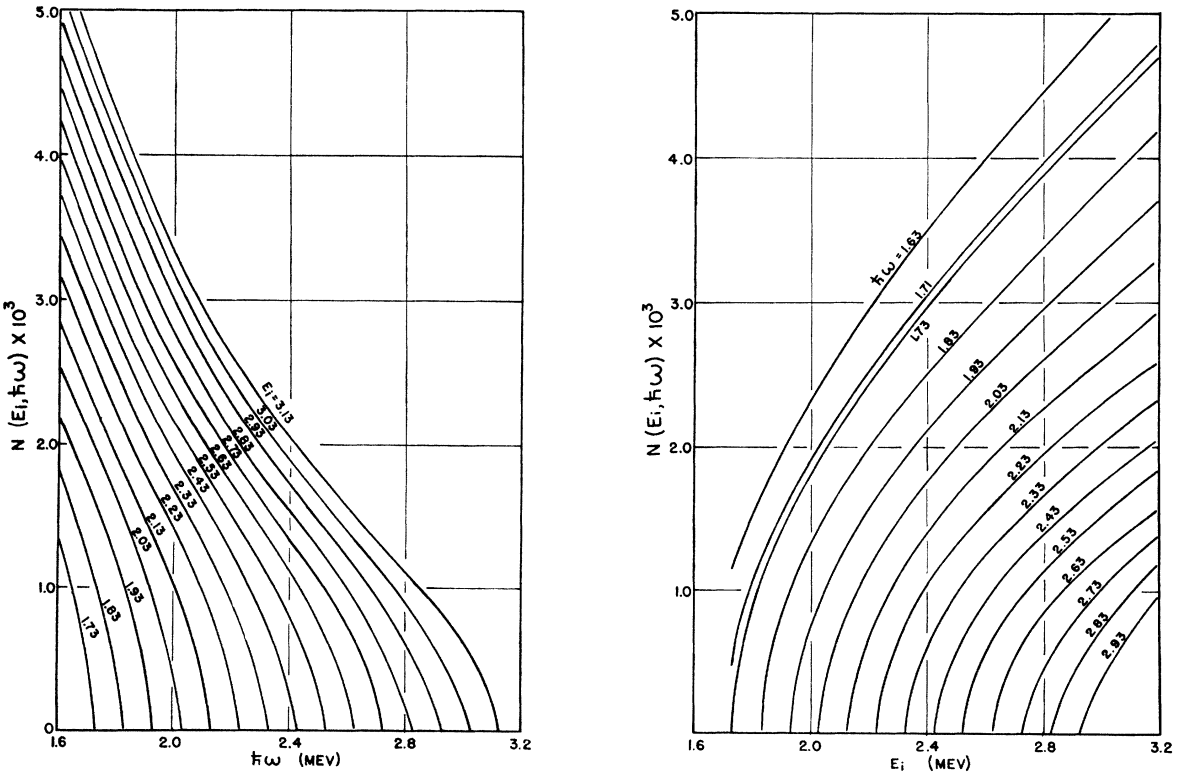

FIG. 7. Number of photomagnetic quanta as a function of $\hbar\omega$ and E_i.

Mev.[2] In the present paper, σ_e will be calculated in terms of $\sigma(\hbar\omega)$ in the energy interval for which only dipole disintegration is important. This procedure, in addition to providing a theory of the electrodisintegration process, yields a correlation between the measured photo-disintegration and electrodisintegration cross sections; this correlation is based upon quantum electrodynamics and is not subject to specific assumptions about the nuclear model employed.

If $\sigma(\hbar\omega)$ is the cross section for photo-disintegration with photons of energy $\hbar\omega$, and $N(E_i, \hbar\omega)$ is the number of photons (per unit energy interval) with energy $\hbar\omega$ by which the action of the field of the electron may be represented in producing the disintegration process, then

$$\sigma_e(E_i)=\int_{\epsilon}^{E_i}\sigma(\hbar\omega)N(E_i,\hbar\omega)d(\hbar\omega), \qquad (38)$$

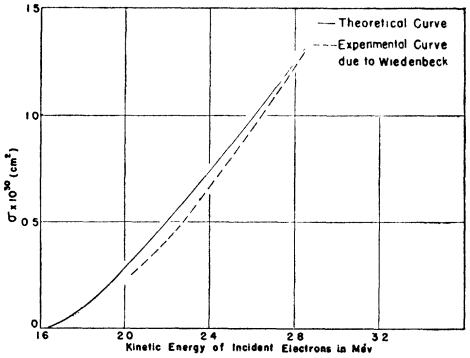

FIG. 8. Electrodisintegration cross sections for Be^9.

where E_i is the kinetic energy of the incident electrons. $N(\hbar\omega, E_i)$ may be evaluated by quantum electrodynamics.[35] For photoelectric disintegration

$$N_e(E_i,\hbar\omega)=\frac{2}{\pi}\frac{e^2}{\hbar c}\frac{1}{\hbar\omega}\left\{\frac{(E_i+mc^2)^2+(E_i-\hbar\omega+mc^2)^2}{2E_i(E_i+2mc^2)}\times\ln\left[\frac{E_i(E_i-\hbar\omega)+mc^2(2E_i-\hbar\omega)+\{E_i(E_i-\hbar\omega)(E_i+2mc^2)(E_i-\hbar\omega+2mc^2)\}^{\frac{1}{2}}}{mc^2\hbar\omega}\right]-\left[1-\frac{\hbar\omega}{E_i}\left(1+\frac{E_i-\hbar\omega}{(E_i+2mc^2)}\right)\right]^{\frac{1}{2}}\right\}, \qquad (39)$$

and for photomagnetic disintegration,

$$N_m(E_i,\hbar\omega)=\frac{2}{\pi}\frac{e^2}{\hbar c}\frac{1}{\hbar\omega}\left\{1-\frac{\hbar\omega}{2E_i}\left[1+\frac{E_i-\hbar\omega}{(E_i+2mc^2)}\right]\right\}\ln\left\{\frac{E_i(E_i-\hbar\omega)+mc^2(2E_i-\hbar\omega)+[E_i(E_i-\hbar\omega)(E_i+2mc^2)(E_i-\hbar\omega+2mc^2)]^{\frac{1}{2}}}{mc^2\hbar\omega}\right\}. \qquad (40)$$

These formulas are derived from the Møller potentials; since the procedure is equivalent to the use of the Born approximation, the formulas (39) and (40) can be expected to yield valid results only if the momentum transferred to the nucleus by the electrons is small compared to their total momentum. However, in view of the difficulties involved in obtaining expressions which are valid for electron energies near the threshold, the formulas (39) and (40) will be applied over the entire energy range covered by the empirical data. Plots obtained from Eqs. (39) and (40) are given in Figs. 6 and 7.

Since the magnetic dipole cross section is negligibly small, only photoelectric disintegration need be considered. Using Eqs. (8), (14), (16), and (39), σ_e may be determined from Eq. (38). The integration cannot be done in closed form in an elementary manner, but numerical evaluation may be carried out readily. Again using the values $V_{1,3/2}=12.16$ Mev, $V_{0,\frac{1}{2}}=V_2=3$ Mev, Eq. (38) yields the electrodisintegration cross section shown as the solid curve in Fig. 8; the dotted curve is a plot of Wiedenbeck's experimental results.

V. DISCUSSION

The results derived in the preceding sections show that the simple two body model of the Be^9 nucleus is adequate for an interpretation of the currently available data on the photo- and electrodisintegration of Be^9. There remains for discussion the correlation between the data on photo- and electrodisintegration and those on disintegration by protons. The sharp maximum observed[4] at 2.41 Mev in the energy distribution of the protons inelastically scattered on Be^9 has been interpreted by Longmire[5] as being due to a $P_{3/2}\rightarrow D_{5/2}$ transition. If this interpretation is correct, this sharp maximum should appear also in the photo-disintegration cross section *versus* energy curve. Unfortunately, the photo cross section has not been measured in the im-

[35] C. Møller, Ann. d. Physik **14**, 531 (1932). See also L. Rosenfeld, *Nuclear Forces* I (Interscience Publishers, New York, 1948), pp. 138–141. The use of the Born approximation to evaluate the number of virtual quanta has been treated in a general way by M. Lax and H. Feshbach (to be published soon). The authors wish to thank Drs. Lax and Feshbach for communicating their results to us.

mediate vicinity of 2.41 Mev, the nearest γ-ray energy being at 2.50 Mev. Because of its extreme sharpness, the maximum may have escaped detection in the photo cross section measurements.

Longmire has chosen the $D_{5/2}$ state as the final state for the following reasons: (1) The virtual levels belonging to states of lower orbital angular momentum are too broad to explain the sharpness of the observed maximum. (2) The D level is presumed to be the lowest energy level which is sufficiently narrow to meet the requirements of the empirical data. The $D_{5/2}$ level is assumed to be of lower energy than the $D_{3/2}$ level; this is to be expected on the basis of relativistic spin-orbit coupling. (3) The matrix elements corresponding to a change of the angular momentum of the incident proton by more than one unit are small. Longmire chooses the well describing the Be^8-neutron interaction in the $D_{5/2}$ state in such a way that the virtual $D_{5/2}$ level is extremely narrow. Unfortunately, the theory of the photodisintegration of Be^9 seems to require that the $D_{5/2}$ level be a broad level centered at an energy considerably higher than 2.41 Mev. A reasonable solution to this problem is to assume the sharp maximum in the proton scattering data to be due to a $P \rightarrow F$ transition. On the assumption that the Be^8-neutron interaction is partly of a Majorana type, it is not at all unreasonable to have the F level at a lower energy than the D level. Furthermore, even though the matrix elements for the $P \rightarrow F$ transition may be small for most energies, a sharp resonance at the narrow F level could result in the sharp maximum observed.

ACKNOWLEDGMENT

The authors wish to thank Mr. G. S. Colladay for the computation of most of the numerical results used in the paper.

PHYSICAL REVIEW VOLUME 76, NUMBER 2 JULY 15, 1949

The (α,n) Cross Section of Boron*

R. L. WALKER**
University of California, Los Alamos Scientific Laboratory, Los Alamos, New Mexico
(Received March 21, 1949)

The differential cross section for the $B^{10,11}(\alpha,n)N^{13,14}$ reactions was measured as a function of the alpha-particle energy up to an energy of 5.3 Mev. To determine this cross section, the number of neutrons emitted by boron under alpha-particle bombardment was measured by comparison with a calibrated Ra-α-Be source in a graphite column.

Resonances were observed at alpha-particle energies of 1.8, 2.5, 4.2, 4.9 Mev. Poor resolution may explain why other resonances found by Maurer and by Fünfer were not observed.

I. INTRODUCTION

NEUTRONS are produced when alpha-particles strike boron, by the two reactions:

$$B^{11}+He^4=N^{14}+n \qquad Q\approx+\ .28 \text{ Mev.}$$
$$B^{10}+He^4=N^{13}+n \qquad Q\approx+1.2 \text{ Mev.}$$

Reasons are given by Bonner and Mott-Smith[1] and by Maurer[2] for believing that only a small fraction of the neutrons from boron (of the order of one-tenth) arise from B^{10}. Thus the principal neutron yield from boron under alpha-particle bombardment is probably due to the first reaction above.

Maurer[2] and Fünfer[3] have studied the $B^{10,11}(\alpha,n)N^{13,14}$ reactions at different alpha-particle energies for the purposes of locating resonances, determining upper limits for their widths and determining the level spacing of the intermediate nucleus for the first reaction, N^{15}.

In the present work an absolute measurement of the cross section for the $B^{10,11}(\alpha,n)N^{13,14}$ reactions was made by determining the number of neutrons emitted from a thin boron target upon which are incident a known number of alpha-particles of variable energy.

II. EXPERIMENTAL ARRANGEMENT

The conventional arrangement shown in Fig. 1 was used as a means of controlling the energy of the alpha-particles striking the boron target. Alpha-particles from polonium coated on the small central sphere, 5 mm in diameter, lose a part of their energy in nitrogen gas before striking the thin boron target coated on the inside of two hemispherical iron spinnings, 7.5 cm in diameter. By changing the pressure of nitrogen in the chamber one can control the energy of the alpha-particles when they reach the boron.

The assembly shown in Fig. 1 was placed in a graphite column containing a sensitive BF_3 proportional counter, in order that the number of neutrons emitted by the

* This paper is based on work performed at Los Alamos Scientific Laboratory of the University of California under contract No. W-7405-eng-36 for the Manhattan Project.
** Now at Cornell University, Ithaca, New York.
[1] T. W. Bonner and L. M. Mott-Smith, Phys. Rev. **46**, 258 (1934).
[2] W. Maurer, Zeits. f. Physik **107**, 721 (1937).
[3] E. Fünfer, Ann. d. Physik **35**, 147 (1939).